In Situ Raman Monitoring of Electrochemical Graphite Intercalation and Lattice Damage in Mild Aqueous Acids

Daniel C. Alsmeyer and Richard L. McCreery*

Department of Chemistry, The Ohio State University, 120 West 18th Avenue, Columbus, Ohio 43210

Simultaneous Raman spectroscopy and electrochemical oxidation of highly ordered pyrolytic graphite (HOPG) permitted monitoring of lattice damage and staging. Intercalation of bisulfate in concentrated H_2SO_4 results in well-known Raman spectral changes in the E_{2g} mode at ca. 1600 cm^{-1}. In addition, damage to the sp^2 lattice is revealed by the "D" band at 1360 cm^{-1}, which occurs when graphitic edges are formed. During oxidation of HOPG in 96% H_2SO_4 or 1 M $NaClO_4/CH_3CN$, intercalation was observed but accompanying lattice damage did not occur at the potentials examined. For 1 M H_3PO_4, neither intercalation nor lattice damage was observed at potentials up to 2.0 V vs SSCE. For 1 M H_2SO_4, 1 M $HClO_4$, or 1 M HNO_3, however, intercalation always preceded or accompanied lattice damage. The results are consistent with a mechanism where oxidation results in a graphite intercalation compound (GIC) which oxidizes either water or the graphite itself to produce carbon oxides. The formation of oxides depends on both the thermodynamic stability of the GIC and the kinetics of intercalation, which in turn correlate with the size of the intercalating ion.

INTRODUCTION

The context of this report is established by work in three rather distinct areas. First, the lattice dynamics of graphite and its intercalation compounds have been examined in detail by the solid-state physics community.[1-11] The Raman spectra of highly ordered pyrolytic graphite (HOPG) and related materials are sensitive to intercalation, with changes in the E_{2g} mode at 1582 cm^{-1} being apparent during intercalation of anions, cations, and neutrals. In this context, "staging" refers to the successive insertion of ions or neutrals between graphite layers, such that "stage V" refers to five layers of graphite between each layer of graphite, stage IV to four layers, etc. An E_{2g}' band appears during intercalation at 1610–1640 cm^{-1} depending on intercalant identity and stage, and this phenomenon has been attributed to "boundary layer" graphite planes adjacent to an intercalant layer.[1] The split in the E_{2g} mode upon intercalation arises primarily from changes in symmetry at the boundary layer and secondarily from electronic effects of the intercalant. In some cases, a quantitative measure of the intercalation stage is available from the E_{2g}/E_{2g}' intensity ratio.

A second area of interest is electrochemical intercalation in nonaqueous solutions or strong aqueous acids.[12-20] Stimulated by work on intercalated batteries, graphite has been oxidized and reduced in numerous solvents, notably Li^+/propylene carbonate and >90% H_2SO_4. Two studies are of direct relevance to this report. Maeda et al.[20] monitored Raman spectra of carbon fibers during cyclic voltammetry in 98% H_2SO_4. They found that 0.0–1.4 V potential cycles did not change the "D" (1360-cm^{-1}) and E_{2g} (1582-cm^{-1}) modes of the fibers. However, a potential excursion to +2.3 V increased the "D" intensity, from which they concluded that the graphite lattice was damaged by intercalation. "Lattice damage" is used here to mean breakup of the extended hexagonal sp^2 array of carbon atoms in graphitic planes and does not refer to intercalation per se. The "D" band results from breakdown of the $k = 0$ selection rule when microcrystallite edges are formed in the graphite lattice.[1,2] A more detailed Raman investigation was undertaken by Eklund et al. on HOPG in 96% H_2SO_4.[21] The cell geometry permitted in situ Raman spectra to be obtained either on the immersed HOPG basal plane or on the basal surface just above the H_2SO_4 during constant-current intercalation. The results showed staging with well-defined 1582- and 1620-cm^{-1} Raman modes. Surprisingly, basal surfaces exhibited rapid electrochemical intercalation, implying that intercalating anions enter the basal surface directly, probably through defects such as cracks, grain boundaries, or step edges. The expected route through edges did not appear operative, in fact lateral migration of HSO_4^- appeared quite slow under the conditions employed. Nishitani et al.[22] monitored changes in the E_{2g} modes observed with spatially resolved Raman spectroscopy for the case where only the *a*-face (i.e. edge plane) of the HOPG was in contact with H_2SO_4. The spatial boundary of Raman spectral changes progressed away from the H_2SO_4 surface as intercalation occurred, at a rate which depended on imposed current density. In contrast to Eklund's conclusions, Nishitani's conditions permitted observation of intercalant diffusion along the *a*-axis.

The third background area of relevance is the large literature on electrochemical pretreatment (ECP) of carbon

* To whom correspondence should be addressed.

(1) Dresselhaus, M. S.; Dresselhaus, G. *Adv. Phys.* **1981**, *30*, 139.
(2) Nemanich, R. J.; Lucovsky, G.; Solin, S. A. *Mater. Sci. Eng.* **1977**, *31*, 157.
(3) Solin, S. A. *Graphite Intercalation Compounds I: Structure and Dynamics*; Springer Verlag: Berlin, 1990; pp 157–219.
(4) Nicklow, R.; Wakabayashi, N.; Smith, H. G. *Phys. Rev. B* **1972**, *5*, 4951.
(5) Al-Jishi, R.; Dresselhaus, G. *Phys. Rev. B* **1982**, *26*, 4514.
(6) Elman, B. S.; Dresselhaus, M. S.; Dresselhaus, G.; Maby, E. W.; Mazurek, H. *Phys. Rev. B* **1981**, *24*, 1027.
(7) Lespade, P.; Al-Jishi, R.; Dresselhaus, M. S. *Carbon* **1982**, *20*, 427.
(8) Nemanich, R. J.; Lucovsky, G.; Solin, S. A. *Solid State Commun.* **1977**, *23*, 117.
(9) Vidano, R. P.; Fischbach, D. B.; Willis, L. J.; Loehr, T. M. *Solid State Commun.* **1981**, *39*, 341.
(10) Nakamizo, M.; Tamai, K. *Carbon* **1984**, *22*, 197.
(11) Eklund, P. C.; Mahan, G. D.; Spolar, J. G.; Zhang, Z. M.; Arakawa, E. T.; Hoffman, D. M. *Phys. Rev. B* **1988**, *37*, 691.
(12) Besenhard, J. O.; Fritz, H. P. *Agnew. Chem., Int. Ed. Engl.* **1983**, *22*, 950.
(13) Kinoshita, K. *Carbon: Electrochemical and Physical Properties*; Wiley: New York, 1988; pp 427–432.
(14) Maeda, Y. *J. Electrochem. Soc.* **1990**, *137*, 3047.
(15) Inagaki, M. *J. Mater. Res.* **1989**, *4*, 1560.
(16) Besenhard, J.; et al. *Synth. Met.* **1983**, *7*, 185.
(17) Fong, R.; VanSacken, U.; Dahn, J. R. *J. Electrochem. Soc.* **1990**, *137*, 2009.
(18) Beck, F.; Krohn, H. *Synth. Met.* **1983**, *7*, 193.
(19) Inagaki, M.; Iwashita, N.; Kouno, E. *Carbon* **1990**, *28*, 49.
(20) Maeda, Y.; Okemoto, Y.; Inogaki, M. *J. Electrochem. Soc.* **1985**, *132*, 2369.
(21) Eklund, P. C.; Olk, C. H.; Holler, F. J.; Spolar, J. G.; Arakawa, E. T. *J. Mater. Res.* **1986**, *1*, 361.
(22) Nishitani, R.; Sasaki, Y.; Nishina, Y. *Synth. Met.* **1989**, *34*, 315.

0003-2700/92/0364-1528$03.00/0

electrodes in milder aqueous media, particularly in the range from pH 0 to 7.[23-34] The bulk of electroanalytical applications of carbon electrodes occur in this pH range, as well as the many examinations of heterogeneous electron transfer and electrochemically initiated homogeneous reactions studied on carbon. As noted by Besenhard in an excellent review,[12] the role of intercalation during ECP of carbon in mildly acidic or neutral solutions is not clear, due to the formation of graphite oxides. The redox potential of graphite intercalation compounds (GIC's) is higher than that for O_2 or CO_2 formation in water, so the GIC is thermodynamically unstable in mild aqueous acids. The result is the formation of the ill-defined electrogenerated graphitic oxide (EGO). Parallel to numerous studies of intercalation, ECP has been used extensively to modify GC and HOPG surfaces, usually for the purpose of electron-transfer activation. Since ECP often leads to large increases in k° for many systems,[23,30,35] an understanding of ECP mechanisms may lead to conclusions about what controls k° at carbon surfaces. Engstrom et al.[23,24] characterized the GC surface following ECP and concluded that surface contaminants were removed by ECP and that the surface becomes hydrophilic. Kepley and Bard[30] used interferometry and elemental analysis to deduce that the film had an approximately 1.5 ratio of oxygen to carbon and that it formed at a rate of about 45 Å per potential sweep (0–1.80 V) in 0.1 M H_2SO_4. Our group used Raman spectroscopy to conclude that ECP of HOPG in mild acid caused breakup of the graphite lattice, and the edges formed are responsible for the increase in electron-transfer rate accompanying ECP.[35,36]

The work reported here was undertaken to complement the numerous electrochemical studies of ECP in mild acid. By simultaneously monitoring Raman spectra and oxidation current during electrochemical pretreatment, we sought to reveal microstructural changes accompanying the electrochemical effects of ECP. Of particular interest are the effects of anion identity in mild aqueous acids.

EXPERIMENTAL SECTION

A diagram of the experimental apparatus is shown in Figure 1. The electrochemical measurements were all performed with a PAR 173 potentiostat which was interfaced with a PC compatible computer (PC). The custom software allowed extremely slow cyclic voltammograms (ca. 1 mV/min). Slow cyclics were achieved by performing a series of small potential steps, to yield the desired average sweep rate. A standard three-electrode system was employed for the electrochemical measurements. The cell was designed so that the platinum-plate auxiliary and the sodium saturated calomel electrodes (SSCE) were separated from the working electrode by a glass frit. The working electrode was a piece of HOPG with the approximate dimensions of 2 mm × 2 mm × 0.1 mm. The mass of this electrode was obtained prior to any electrochemical modification. This small electrode was held in place by two pieces of platinum plate which were fused in a fashion such that they formed a clamp to hold the electrode. The working electrode was inserted into the glass cell such that the impinging laser beam could enter the cell and excite the basal plane region of the exposed HOPG while the scattered radiation was collected and focused on the spectrograph entrance slit. Both basal and edge surfaces of the HOPG sample were exposed to the solution.

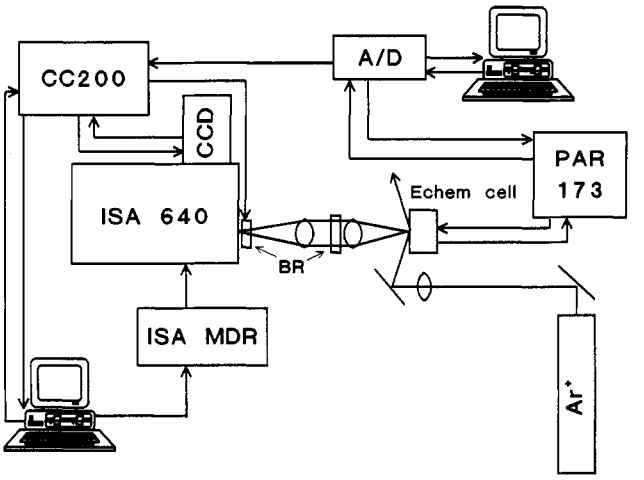

Figure 1. Schematic of experimental apparatus. Abbreviations: CC200, CCD detector; PAR, Princeton Applied Research potentiostat; BR, band reject filter; MDR, motor controller; A/D, computer interface and digitizer.

Raman measurements were performed on an Instruments SA 640 single monochromator equipped with a 300 line/mm grating operating in second order with a Photometrics PM512 charge-coupled device (CCD) detector.[37] The CCD was interfaced to a second PC to control spectral acquisition and store spectra. Dielectric band reject interference filters[37] were placed near the entrance slit and collimating lens to reject the Rayleigh scattered light. An argon ion laser operating at 514.5 nm was used to illuminate the sample with approximately 100 mW of laser power at the laser head. The CCD detector was cooled with liquid nitrogen to −110 °C. The CCD was exposed to the scattered light for integration times varying from 100 to 600 s. The Raman shifts were calibrated using a neon bulb before each set of measurements. The software permitted automatic spectral acquisition at any point in a potential scan or step via a trigger from the electrochemical PC to the CCD computer. Thus the spectral and current vs potential results could be obtained automatically and simultaneously.

RESULTS

Raman spectral changes accompanying intercalation in concentrated H_2SO_4 were observed initially, in order to characterize a well-behaved system and to provide baseline data in the absence of carbon oxide formation. A slow-scan cyclic voltammogram for HOPG in 96% H_2SO_4 is shown in Figure 2, with the potential axis unfolded for clarity. The large oxidation peak at ca. 1.2 V vs SSCE is the stage II to stage I transition, while the current in the 0.6–0.9-V potential range is composed of overlapping peaks for stage V to stage II transitions. The electrochemical results are similar to those reported by Besenhard et al.[12] At positive potentials the HOPG sample expanded and turned blue due to intercalation of HSO_4^- and accompanying H_2SO_4. Since this process has been reported in detail in the literature, only the Raman results will be discussed further here.

Figure 3 shows Raman spectra of the E_{2g} region obtained at various points in the oxidation scan of Figure 2. When the potential remained below 1.5 V, no D band at 1360 cm^{-1} was apparent at any time. Raman shifts are also plotted in Figure 2 for the E_{2g} and E_{2g}' bands. Note that the "boundary layer" mode at ca. 1620 cm^{-1} is clearly visible next to the E_{2g} mode for the potential range from 0.658 to 0.762 V vs SSCE. At

(23) Engstrom, R. C.; Strasser, V. A. *Anal. Chem.* **1984**, *56*, 136.
(24) Engstrom, R. C. *Anal. Chem.* **1982**, *54*, 2310.
(25) Kovach, P. M.; Deakin, M. R.; Wightman, R. M. *J. Phys. Chem.* **1986**, *90*, 4612.
(26) Wang, J.; Hutchins, L. O. *Anal. Chim. Acta* **1985**, *167*, 325.
(27) Cabaniss, G. E.; Diamantis, A. A.; Murphy, W. R., Jr.; Linton, R. W.; Meyer, T. J. *J. Am. Chem. Soc.* **1985**, *107*, 1845.
(28) Falat, L.; Cheng, H. Y. *J. Electroanal. Chem. Interfacial Electrochem.* **1983**, *157*, 393.
(29) Gonon, F. G.; Fombarlet, C. M.; Buda, M. J.; Pujol, J. F. *Anal. Chem.* **1981**, *53*, 1386.
(30) Kepley, L. J.; Bard, A. J. *Anal. Chem.* **1988**, *60*, 1459.
(31) Gewirth, A. A.; Bard, A. J. *J. Phys. Chem.* **1988**, *92*, 5563.
(32) Bowling, R. J.; Packard, R. T.; McCreery, R. L. *Langmuir* **1989**, *5*, 683.
(33) McCreery, R. L. In *Electroanalytical Chemistry*; Bard, A. J., Ed.; Dekker: New York, 1991; Vol. 17, pp 221–374.
(34) Nagaoka, T.; Yoskhino, T. *Anal. Chem.* **1986**, *58*, 1953.
(35) Bowling, R.; Packard, R.; McCreery, R. L. *J. Am. Chem. Soc.* **1989**, *111*, 1217.
(36) Alsmeyer, Y. W.; McCreery, R. L. *Langmuir* **1991**, *7*, 2370.
(37) Alsmeyer, Y. W.; McCreery, R. L. *Anal. Chem.* **1991**, *63*, 1289.

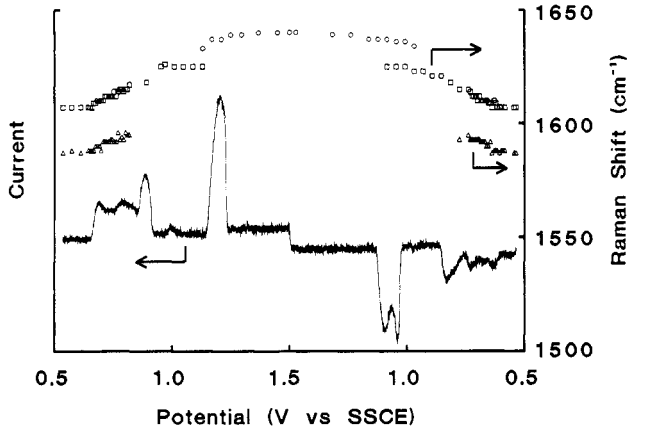

Figure 2. Current and Raman shifts during intercalation of HOPG in 96% H_2SO_4. The scan rate was 1 mV/min. Triangles indicate the E_{2g} band, squares and circles indicate E_{2g}'. Note scan reversal at 1.5 V.

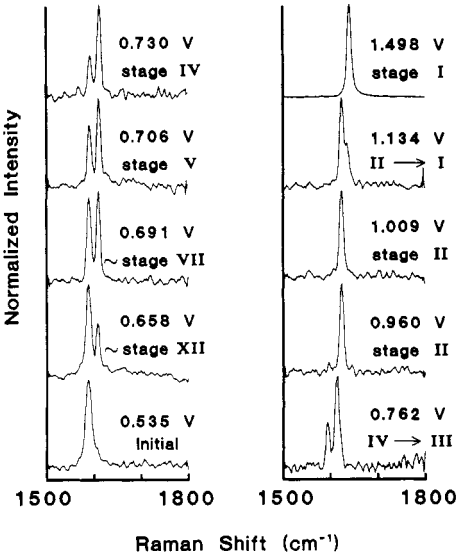

Figure 3. Raman spectra of E_{2g} region acquired during voltammetric scan from Figure 2. Stage numbers were deduced from the E_{2g}/E_{2g}' ratio (Figure 4). Intensities were normalized to maximum values for each spectrum.

0.960 and 1.009 V, only stage II is present (two graphite layers alternating with one intercalant layer), so every graphite layer is a boundary layer and only one peak is observed. A further increase in Raman shift occurs in the transition from stage II to I. Plots of Raman shift vs the inverse of the stage number are linear for both the E_{2g} and E_{2g}' bands, as noted by Dresselhaus and others.[1,3] Figure 4 shows that ratio of the E_{2g} and E_{2g}' bands is linear with stage number, as would be expected if E_{2g}' is derived from boundary layers. Although the slope of this line depends on relative cross sections for E_{2g} and E_{2g}' scattering, smaller values of the ratio indicate higher stage number. The spectra of Figure 3 were normalized to permit easy comparison, but the absolute intensity of the spectra increased during intercalation by a factor of 25 from the initial E_{2g} intensity to the final E_{2g}' intensity. As noted by Maeda et al.[20] and Eklund et al.,[21] oxidation of HOPG or carbon fibers above 1.5 V leads to lattice damage indicated by the "D" band.

While concentrated H_2SO_4 electrolyte leads to well-behaved intercalation, it is not very relevant to electroanalytical and ECP experiments. A series of 1 M aqueous electrolytes was examined with both voltammetry and Raman spectroscopy to consider intercalation under milder conditions. The choice of electrolyte was dictated in part by resistance to oxidation. For example, Cl^- is oxidized at potentials lower than that required for intercalation, so HCl and KCl were not studied.

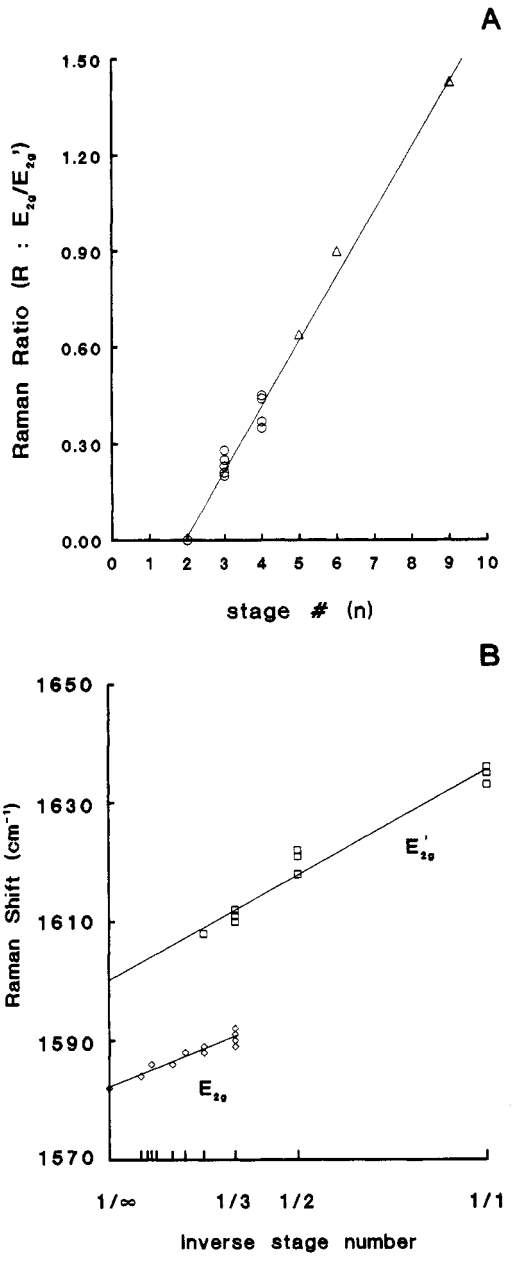

Figure 4. (A) E_{2g}/E_{2g}' integrated Raman intensity ratio vs stage number deduced from voltammetry and charge/mass ratio. (B) Raman frequencies plotted vs inverse stage number for intercalation in 96% H_2SO_4.

From the standpoint of feasibility and previous data from the literature, 1 M solutions of H_2SO_4, $HClO_4$, HNO_3, and H_3PO_4 in water were examined, as was 1 M $NaClO_4$ in acetonitrile.

Figure 5 shows a slow-scan voltammogram of HOPG in 1 M $HClO_4$ with the current integrated to reduce noise and stated as a charge per unit mass of HOPG. Oxidation is evident at ca. +0.8 V vs SSCE, and large currents are present above 1.0 V. Raman spectra obtained at selected potentials during the experiment depicted in Figure 5 are shown in Figure 6. The D band and a distorted E_{2g}' mode are readily apparent at 1.580 V, and some D band intensity is visible at 1.439 V. Figure 6B shows difference spectra of the E_{2g} region at several potentials relative to the spectrum observed at 0.500 V. Changes in the E_{2g} band are apparent at 1.118 V, which increase with potential. Figure 5 includes the E_{2g}'/E_{2g} intensity ratio obtained simultaneously with the voltammetric data. Due to inaccuracies in measuring the E_{2g}'/E_{2g} ratio in Figure 5, the apparent fluctuations in the ratio may not be real. However, the onset and general increase in the ratio

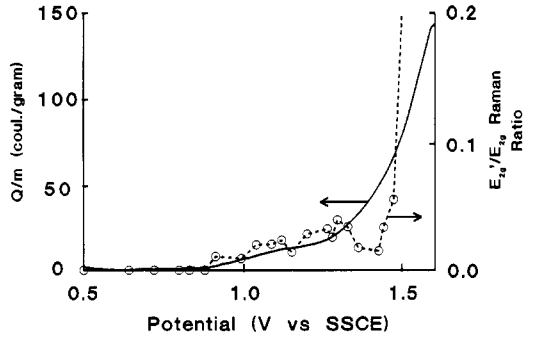

Figure 5. E_{2g}/E_{2g}' Raman intensity ratio (dashed line) and charge/mass ratio (solid line) for intercalation of a 0.1- × 2- × 2-mm HOPG sample in 96% H_2SO_4.

with potential are reproducible. Figures 5 and 6 both indicate that changes in the E_{2g} mode precede observable D band intensity.

Figures 7–9 were taken from potentiostatic pretreatment where the potential of interest was applied for 2 min, with simultaneous acquisition of a Raman spectrum. Spectra for HOPG pretreated at various potentials are shown for three electrolytes in Figure 7. The spectra for 1 M H_2SO_4 and 1 M HNO_3 are qualitatively very similar to those for 1 M $HClO_4$. Note that H_3PO_4 does not intercalate to an observable extent up to 2.0 V, while HNO_3, $HClO_4$, and H_2SO_4 cause obvious intercalation and lattice damage at 1.5–1.7 V. The D/E_{2g} and E_{2g}'/E_{2g} intensity ratios are plotted in Figures 8 and 9 for potentiostatic pretreatment in five electrolytes.

Several useful observations are available from the results shown in Figures 5–9. First, the nature of intercalation in mild electrolytes is strongly dependent on the solvent and salt identities. H_2SO_4, $HClO_4$, and HNO_3 (all 1 M) are qualitatively similar, while $NaClO_4/CH_3CN$ shows intercalation but no lattice damage (indicated by the D band), and H_3PO_4/H_2O shows neither intercalation nor lattice damage. Second, the onset potentials of both intercalation and lattice damage depend strongly on the electrolyte, on the basis of the E_{2g}' and D intensities shown in Figures 8 and 9. Listed in order of decreasing propensity to cause changes in the D and E_{2g} bands, the 1 M electrolytes are $HNO_3 > HClO_4 > H_2SO_4 > NaClO_4/CH_3CN \gg H_3PO_4$. The onset potentials for both the E_{2g}' and D bands are listed in Table I, along with the intensity ratios reached at 2.00 V.

DISCUSSION

Intercalation and related structural changes in HOPG depend on several variables, including site and rate of initial ion insertion between layers, mass transport of intercalants into the bulk lattice, thermodynamic potential of various stages for different intercalants, intraplanar lattice damage, and carbon oxidation to form graphitic oxide, CO_2, etc. Although these factors have been examined in significant detail, the relative importance of each effect in a given experiment depends greatly on conditions. In addition to revealing structural changes during intercalation using Raman spectroscopy, our purpose here is to use conditions similar to those present in the numerous applications of carbon electrodes in analysis and synthesis. The multichannel Raman spectrometer used here to monitor intercalation in situ is particularly valuable, since it provides rapid spectra in real time, simultaneously with intercalation.

Before turning to mild aqueous electrolytes, the results in 96% H_2SO_4 provide useful observations. This medium suppresses oxide formation due to low water activity, so intercalation can proceed to a low stage index without complication from side reactions. Of interest is the immediate (≤2 min) onset of Raman spectral changes to the E_{2g} band even when the laser beam is positioned on the HOPG basal surface far away (1 mm) from edges. If intercalation occurred solely through the cut edge of the sample (the "*a*" face), there should be a lag before the E_{2g}' band is observed in the center of the sample. As noted by Nishitani et al.,[22] such a delay occurs when only the *a*-face is immersed in H_2SO_4. In fact, a front corresponding to a stage transition progresses away from the H_2SO_4/*a*-face junction as intercalant diffuses into the sample. When the entire sample is immersed (as was the case here) intercalation is rapid near or far from the *a*-face and then propagates into the sample interior. This observation is consistent with intercalant entry through defects and crystallite boundaries on the basal surface. X-ray results indicate a microcrystallite size of ca. 10 μm for HOPG,[33] and numerous step edge defects are observed with STM. Assuming intercalation begins at such defects, the intercalant need only diffuse a few microns to completely intercalate the basal surface. It should be noted that differences in intercalation dynamics may well result from sample-dependent parameters such as microcrystallite size and long-range order.

On the basis of the optical properties of HOPG, the combination of beam penetration and scattered photon escape depth results in a Raman sampling depth of about 130 Å.[37] Intercalation compounds have lower graphite density and different optical properties than the initial HOPG, so one might expect the sampling depth to be greater. On the basis of Figures 3 and 4A, the cross section for boundary layer graphite (E_{2g}') is about 2.5 times that of the inner layer (E_{2g}), at least for HSO_4^- intercalation. For example, the stage IV GIC in Figure 3 exhibits a stronger E_{2g}' peak for an equal number of inner and boundary layers. Since intercalation to stage I yields a 25-fold increase in scattering intensity (for E_{2g}' compared to unintercalated E_{2g}), the Raman sampling depth for the stage I GIC must have increased by a factor of ca. 10 (to about 1500 Å) compared to unmodified HOPG.

The data of Figures 2–4 permit an assessment of stage number from Raman frequencies and intensities, provided the scan rate (1 mV/min in this case) is slow enough to permit intercalation to occur throughout the HOPG sample. Since equilibration can occur, the slow-scan results should reflect the thermodynamic stability of different GIC's, provided intercalation is the only process occurring. Besenhard and Fritz[38] and Rudorff and Hofmann[39] report that the GIC's formed in $HClO_4$ or H_2SO_4 are more stable toward oxide formation than that in HNO_3, which is in turn more stable than that from H_3PO_4. In other words, the reduction potentials for $HClO_4$ and H_2SO_4 GIC's are lower than HNO_3 and H_3PO_4 GIC's, and their thermodynamic propensity to form oxides is lower. Beck et al.[40] reported a quasireversible potential for intercalation of natural graphite flakes which decreased with increasing H_2SO_4 or $HClO_4$ concentration. It is not surprising that intercalation is "easier" for more concentrated intercalants, but the relationship between potential and concentration was not Nernstian. Thus the main thermodynamic conclusion available from slow-scan experiments in concentrated acids is that intercalation occurs at lower potentials for more concentrated acids, and the order of reduction potential is $H_3PO_4 \gg HNO_3 > H_2SO_4 \simeq HClO_4$. Since oxide formation is thermodynamically unfavorable in concentrated acids and since intercalation is permitted to reach equilibrium due to the slow-scan rate, the Raman results reflect the order of reduction potentials of the respective GIC's.

Conclusions about intercalation and lattice damage in mild aqueous acids are best divided into qualitative observations distinguishing different intercalants and more quantitative issues regarding onset potentials and intercalation rates.

(38) Besenhard, J. O.; Fritz, J. P. *Z. Anorg. Allg. Chem.* **1975**, *416*, 106.
(39) Rudorff, W.; Hoffmann, U. *Z. Anorg. Allg. Chem.* **1938**, *238*, 49.
(40) Beck, F.; Junge, H.; Krohn, H. *Electrochim. Acta* **1981**, *26*, 799.

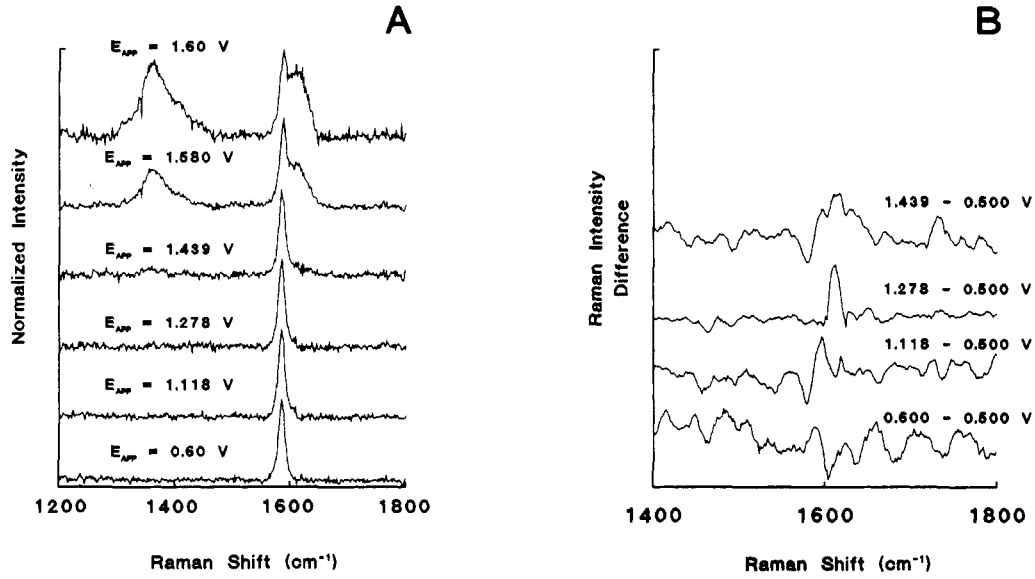

Figure 6. (A) Raman spectra of HOPG obtained during a slow scan from 0.50 V to various potentials in 1 M $HClO_4$. (B) Difference spectra of the E_{2g} region, referenced to 0.500 V. Intensities of both sets of spectra were adjusted for comparison but varied only slightly from run to run.

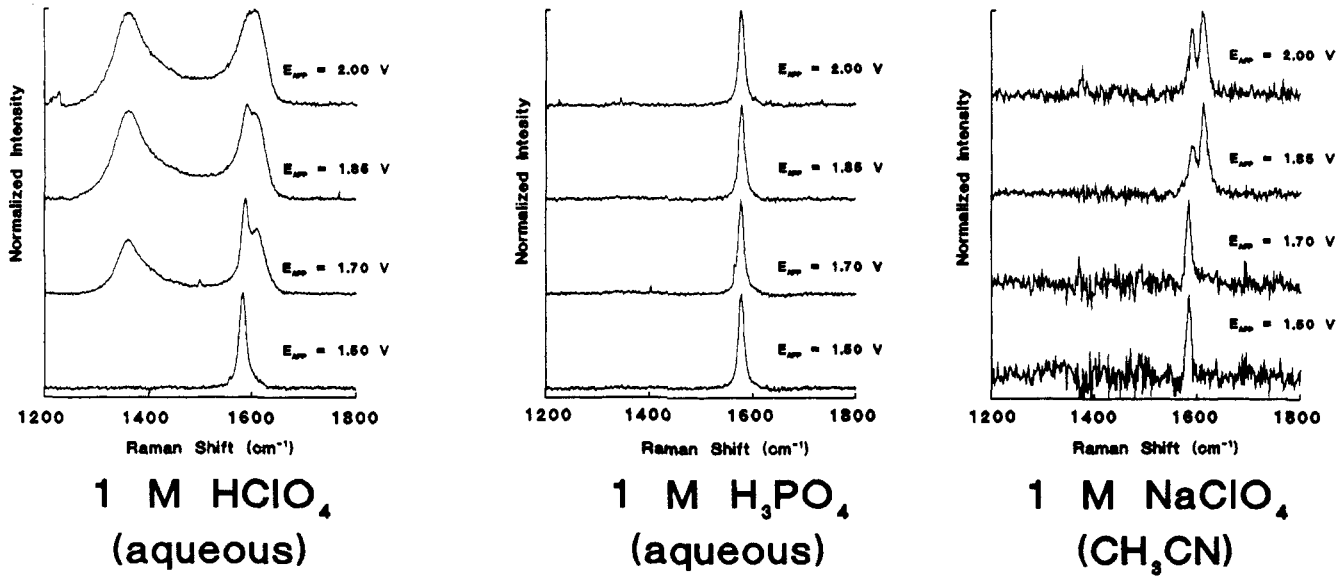

Figure 7. Raman spectra of HOPG after potential steps lasting 2 min from 0.500 V to four potentials in 1 M $HClO_4$, 1 M H_3PO_4, and 1 M $NaClO_4/CH_3CN$. Baseline noise in the CH_3CN case was due to subtraction of solvent bands.

Referring to Figure 7, several qualitative conclusions are available. First, lattice damage as indicated by the D band was always preceded or accompanied by intercalation. In no case did breakup of the sp^2 lattice occur without evidence of accompanying intercalation. Of particular note is 1 M H_3PO_4, when neither intercalation nor lattice damage occurred at potentials up to and including 2.00 V vs SSCE. Second, it was possible to intercalate without lattice damage, in the case of $NaClO_4/CH_3CN$ or 96% H_2SO_4. Thus intercalation per se does not cause lattice damage, but rather an associated or subsequent process. Third, in all cases studied where intercalation occurred in mild aqueous acids (1 M HNO_3, 1 M $HClO_4$, 1 M H_2SO_4), lattice damage resulted. These qualitative conclusions indicate a sequence of events in which intercalation occurs if favorable; then the intercalation compound undergoes chemical reactions leading to lattice damage under certain conditions. In CH_3CN or 96% H_2SO_4, the intercalation compound is stable toward these chemical reactions so damage does not occur, and in 1 M H_3PO_4, intercalation and any subsequent lattice damage were not observed. The evidence indicates that the intercalation compounds formed in mild aqueous acids rapidly form oxides, a process which generates enough strain to result in lattice damage and appearance of the "D" band.

Although based on different evidence obtained in different media, a mechanism based on intercalation followed by lattice damage and oxide formation was concluded by Besenhard et al.[12] and Beck et al.[40] for mild aqueous acids. As the acid strength decreases, the reduction potential for intercalation *increases*, in some cases linearly. Thus weaker acids lead to a higher potential for formation of intercalation compounds. Furthermore, CO, CO_2, O_2, and graphite oxide formation occur at *lower* potentials as the acid concentration decreases. Thus solely on thermodynamic grounds, the potential for intercalation will become more positive than the potential for oxide formation as the acid strength is decreased. The spectral data of Figure 7 indicate that although the intercalation compound is unstable in 1 M HNO_3, $HClO_4$, or H_2SO_4, it does form before or simultaneously with lattice damage. Conversely, without intercalation (as in 1 M H_3PO_4), no lattice damage is observed even at high potentials. This mechanism is also consistent with that proposed earlier, in which oxide formation on carbon edges creates strain which results in lattice damage.[32] Such a process is also consistent with the nucleation and growth mechanism concluded from STM[31] and Raman microprobe[35] observations. The results presented

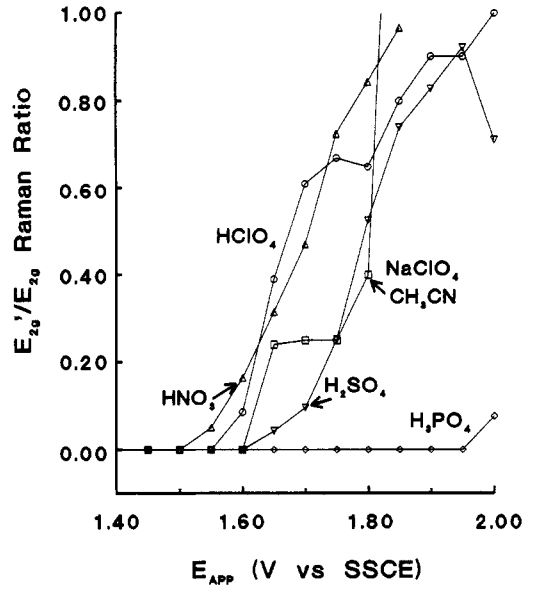

Figure 8. E_{2g}'/E_{2g} integrated intensity ratio for HOPG in five electrolytes: Triangles, HNO_3; circles, $HClO_4$; squares, $NaClO_4/CH_3CN$; inverted triangles, H_2SO_4; diamonds, H_3PO_4. Spectra were acquired during successive potential steps to E_{app}. All electrolyte concentrations were 1 M in water, except for 1 M $NaClO_4$ in CH_3CN.

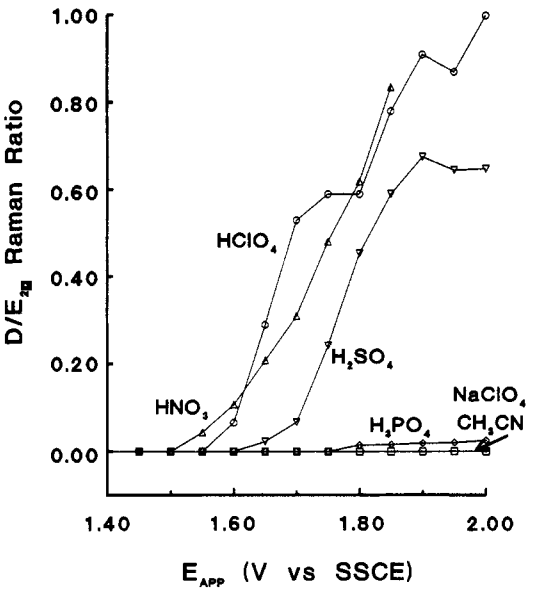

Figure 9. Integrated D/E_{2g} intensity for five electrolytes, otherwise same as Figure 8.

Table I. Raman Peak Intensity Ratios after ECP in 1 M Electrolytes

	D/E_{2g} E_{app} = 2.00 V	E_{2g}'/E_{2g} E_{app} = 2.00 V	D band onset, potential steps[b]	E_{2g}' onset, slow scan[b]
H_2SO_4/H_2O	0.65	0.71	1.65	1.0–1.1
$HClO_4/H_2O$	1.0	1.0	1.60	0.9–1.0
HNO_3/H_2O	0.83 (1.85 V)	0.96 (1.85 V)	1.55	1.1–1.2
H_3PO_4/H_2O	0.025	0.077	>1.80	–[a]
$NaClO_4/CH_3CN$	0.00	1.28	–	–

[a] A dash indicates that no band was observed. [b] Volts vs SSCE.

here add to these previously reported mechanisms the new information that intercalation of HOPG always precedes lattice damage and presumably oxide formation.

The quantitative aspects of intercalation and lattice damage reveal further factors which control the process. On the basis of the onset of the E_{2g}' and D bands noted in Figures 8 and 9 and Table I, 1 M HNO_3 is a more aggressive medium than the other dilute acids studied. On the basis of lattice damage and E_{2g}' appearance, the relative order of electrolytes is HNO_3 > $HClO_4$ > H_2SO_4 ≫ H_3PO_4. Although $HClO_4$ has been reported to be the thermodynamically most favorable intercalant of the group,[39] HNO_3 shows intercalation and lattice damage at lower potentials in mild media. Apparently, a kinetic factor is involved for conditions other than a very slow scan rate. Since carbon oxide formation accompanies intercalation in mild acids, the rate of intercalation relative to oxide formation may be important and a thermodynamic limit may never be reached. $HClO_4$ may be thermodynamically favored to reach a particular stage number at a lower potential than HNO_3, but the more rapid kinetics of NO_3^- intercalation lead to both E_{2g}' intensity and lattice damage at potentials lower than predicted on solely thermodynamic grounds.

Table II. Radii of Selected Anions

anion	ionic radius (pm)	hydrated radius (pm)[a]
ClO_4^-	189	350
SO_4^{2-}	236	400
NO_3^-	230	300
PO_4^{3-}	238	400
HPO_4^{2-}		400
$H_2PO_4^-$		450

[a] Debye Huckel ion size parameter.[41]

The ionic and hydrated radii for the anions studied are listed in Table II. Intercalation has been observed for both solvated and unsolvated anions,[12] and the data presented here do not indicate which occurs in dilute acids. However, for the monoanions concerned, the onset potential for lattice damage is lower for smaller ionic or hydrated radii. Not surprisingly, the smaller ions are more aggressive toward intercalation.

Conclusions about intercalation based on HOPG in mild acid should apply to carbon materials with comparable d_{002} spacing (3.35 Å) such as pyrolytic graphite, spectroscopic graphite rods, and many vapor-deposited carbon films. These materials are less ordered than HOPG, and their higher density of graphitic edges may accelerate oxide formation relative to intercalation, possibly leading to lower sensitivity to anion identity. As d_{002} increases, intercalation behavior may differ. Of particular interest is glassy carbon with a d_{002} of ca. 3.6 Å and much less microcrystalline order than HOPG. GC intercalation, if it occurs at all, has not been studied in detail, and GC is not as amenable to the Raman technique used here because the E_{2g}' and E_{2g} bands are not well resolved. The absence of detectable sulfur in graphite oxide formed during ECP of GC in 0.1 M H_2SO_4[30] implies either that intercalation of HSO_4^- into GC does not occur or that HSO_4^- is lost upon lattice damage and oxide formation.

In summary, the behavior of HOPG upon oxidation in mild aqueous acids is strongly dependent on the identity of the anion. If intercalation does not occur (as for 1 M H_3PO_4), no changes in the HOPG were observed. If intercalation does occur, the process might be reversible with no damage to the sp^2 lattice (as with $NaClO_4/CH_3CN$ or 96% H_2SO_4). If intercalation occurs and oxide formation is thermodynamically favorable, lattice damage occurs (e.g. 1 M $HClO_4$, H_2SO_4, or HNO_3). Oxide formation is a function of both thermodynamic and kinetic effects, and the rate of intercalation and subsequent lattice damage appears to be higher for smaller intercalating ions.

ACKNOWLEDGMENT

This work was supported by the Analytical and Surface Chemistry Division of the National Science Foundation.

RECEIVED for review January 6, 1992. Accepted April 23, 1992.

(41) Kielland, J. *J. Am. Chem. Soc.* **1937**, *59*, 1675.